A Reliable Approach for Evaluating the Platform Tolerance of RFID Tag Antennas

Li Li[1,2,3] and Raj Mittra[3]

[1] Electromagnetic Communication Laboratory, Communication University of China
1307 Yifu Bldg, Communication University of China, Beijing, 100024 China

[2] Information Engineering School, Communication University of China
1st Floor Main Bldg, Communication University of China, Beijing, 100024 China
racky@cuc.edu.cn

[3] Electromagnetic Communication Laboratory, Pennsylvania State University
319 EE East, University Park, PA 16802 USA
rajmittra@ieee.org

Abstract—This paper describes a novel approach for evaluating the performance of an RFID tag on the basis of the simulation of its input impedance. A systematic and reliable approach to compute the impedance is presented and the platform tolerance characteristics of two tags are investigated on the basis of the variations of their input impedances.

Index Terms—Radio frequency identification (RFID), finite difference time domain (FDTD), planer inverse F antenna (PIFA) tag, meander tag, coax feed.

I. INTRODUCTION

Recent years have witnessed the use of Radio Frequency Identification (RFID) systems for a wide variety of applications, such as tracking and inventory control. The RFID reader uses the backscattered field from a tag, typically operating at or near the frequencies of 915MHz and 2.4GHz. Other frequencies, such as 125 kHz and 13.56 MHz, are also used in some systems, which rely on near-field communication technology [1-2]. The system is comprised of a reader, which includes an antenna, and the tag (also referred to as a transponder) that contains the tag antenna and a chip which stores the ID data. The antenna is designed to have an impedance which is different from the usual 50 Ω, so that it can provide a conjugate match to the chip impedance, which usually has a small resistive part accompanied by a relatively large reactance, typically 140Ω, or even higher.

An important attribute as well as performance metric of an RFID tag is its read range. Typically we use the modified Friis equation below to compute the read range,

$$r = \frac{\lambda |a_r \cdot a_t|}{4\pi} \sqrt{\frac{EIRP \, G_t G_r (1-|\Gamma_t|^2)(1-|\Gamma_r|^2)}{P_{th}}}, \quad (1)$$

where, a_t and a_r are the polarization vectors of the reader and tag antennas, respectively, and λ is the wavelength of the operating frequency. EIRP stands for equivalent isotropically radiated power, (usually 4 W). G_t and G_r are the gains of the reader and tag antennas, respectively. Γ_t and Γ_r are reflection coefficients of the reader and tag antennas, respectively. P_{th} is the threshold of tag antenna, which is usually a design parameter of the tag chip.

When the tag is placed on different types of platforms, e.g., cardboard, plastic, glass or metal, the read range of the tag is affected, because its

resonant frequency, input impedance, gain, etc. vary with the change in its environment. In [3], the authors also state that: "The differential RCS of an RFID tag is an important parameter which determines the power of the modulated backscattered signal." The differential RCS, in turn, can be affected by a change in the input impedance; hence, it is important to study the input impedance behavior of an RFID tag, especially when it is mounted on different platforms.

In this paper, we present a systematic approach for estimating the tolerance of a tag when its environment is modified. We show that this information, which is very helpful at the design stage of a tag, can be obtained in a reliable way — even when the tag is placed on different platforms — by estimating the impedance of the antenna. Conventional models of the feed used by most CEM codes render the impedance estimate to be highly sensitive to the geometry of the feed region. This is evidenced by the fact that different computational codes using different feed models often yield widely varying results. This is partly due to the fact that the real part of the input impedance of the tag is relatively small, and the slope of the reactance is large at the operating frequency of the tag. Regardless of the CEM codes used, the results for the impedances can be inaccurate when the impedance is evaluated in the feed region where the higher-order modes are present. Specifically, measuring the voltage and current directly at the feed point in the presence of the higher-order modes can corrupt the results and yield non-physical values for the input impedance, e.g., one with a negative real part for a passive tag.

Consider, for instance, the case of a PIFA tag fed with a short coax as shown in Fig. 1(a). The red line in the coax indicates the excitation point, while the voltage and current measurement points are marked in blue. Figure 1(b) shows that the

input impedance is non-physical above 970MHz, because the real part of the impedance is negative, most likely because of the presence of the higher-order modes. In this work, we employ a longer
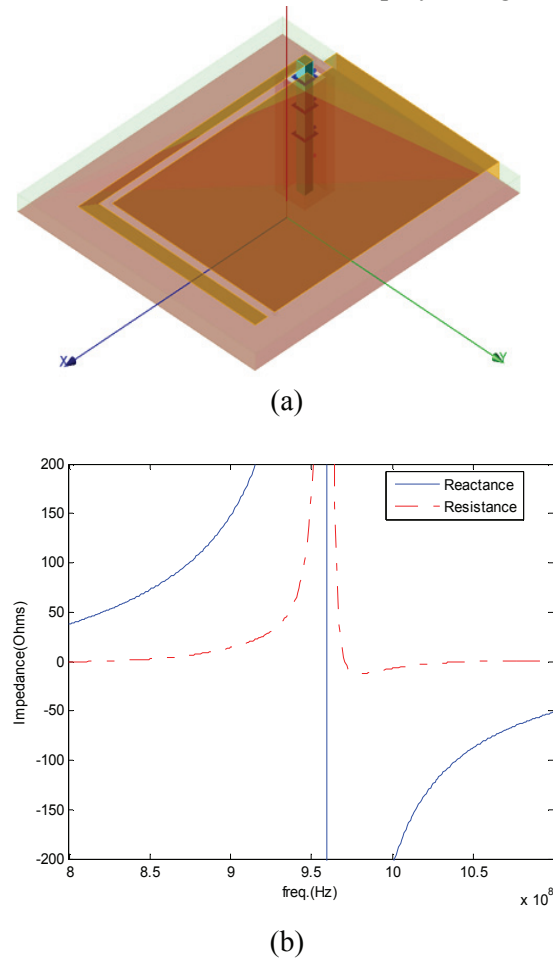

(a)

(b)

Fig. 1. Nonphysical results obtained when a short coax used to feed a PIFA tag: (a) Geometry of short coax feeding a PIFA tag; (b) Input impedance.

coax transmission line feed to obviate the above problem when computing the input impedance and evaluating the efficiency of power delivered to the chip embedded in the tag. Note that this alternate approach mimics the real-life measurement with a Vector Network Analyzer (VNA), and has been found to consistently yield realistic results.

We employ GEMS [4], a general-purpose EM solver, which has been parallelized for handling

complex EM problems in a time-efficient manner. As mentioned earlier, we use a coaxial line to feed the tag, as we would when measuring the return loss characteristic of a device using a VNA. We note that such a configuration is not handled easily by using the MoM-based commercial codes because of the nature of the Green's function used in the formulation of the numerical problem in such a code. Though the finite methods do not suffer from this drawback, they can, nonetheless, become burdensome in terms of CPU time and memory when modeling the tag-coax composite on a single PC. GEMS overcomes this problem by using a parallelized code, which scales with better than 90% efficiency, even on a large number of processors [4].

II. EVALUATION OF TAG IMPEDANCE USING A COAXIAL FEED

To evaluate the impedance of the tag we use the FDTD code to measure the voltage or current distributions along the feed line. Figure 2 shows a model of the structure simulated by using GEMS, where red indicates the outer part of the coax; the outputs of the voltage and current are plotted in blue; and black is the inner part of coax. The length of coax is chosen to be on the order of λmax of the frequency band of interest — typically, we choose this length to be at least $2/3\lambda_{max}$ — so that we can capture at least one maximum and one minimum of the standing wave
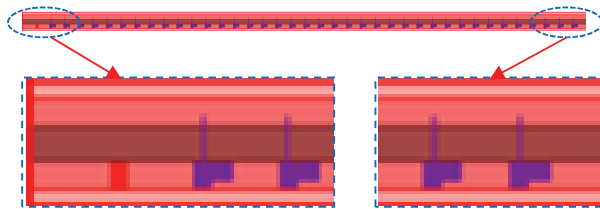

Fig. 2. Geometry of the longer coax simulated in GEMS with measurement points indicated in the figure. Coax' length is 200mm and the inner and outer diameters of the coax are 2mm and 5.08mm, respectively.

distribution in the coax. This enables us to evaluate the reflection coefficient of the TEM mode, without it being affected by the presence of the higher-order modes, which inevitably exist in the vicinity of the feed point.

The knowledge of Γ, the locations of the maxima and the minima of the standing waves, and the characteristic impedance Z_C of the coax enables us to compute the tag impedance by using the well known formulas, given below:

$$\Gamma = \frac{Z_L - Z_C}{Z_L + Z_C}, \tag{2}$$

where, Γ is reflection coefficient, and Z_L and Z_C are the load and characteristic impedances of the coax, respectively. Next, we obtain the SWR from:

$$SWR = \frac{V_{max}}{V_{min}} = \frac{I_{max}}{I_{min}} = \frac{1 + |\Gamma|}{1 - |\Gamma|}. \tag{3}$$

From (2) and (3), we can get

$$Z_L = Z_C \frac{1 + \Gamma}{1 - \Gamma} = Z_C \frac{1 + |\Gamma|e^{j\theta}}{1 - |\Gamma|e^{j\theta}}, \tag{4}$$

where, $\theta = \beta * d$ and d is the distance from load, and

$$|\Gamma| = \frac{SWR - 1}{SWR + 1}. \tag{5}$$

Note that form (4) we can obtain the Z_{Lmax} and Z_{Lmin} by setting $\theta = 0$ and $\theta = \pi$, respectively. The relevant equations are:

$$Z_{Lmax} = Z_C \frac{1 + |\Gamma|}{1 - |\Gamma|} \tag{6}$$

$$Z_{Lmin} = Z_C \frac{1 - |\Gamma|}{1 + |\Gamma|}. \tag{7}$$

We can easily determine the locations of Z_{Lmax} and Z_{Lmin}, by determining the location of the voltage and current maxima along the coax, which yield dmax and dmin, respectively. Finally, we can drive Z_L by using

$$Z_L = Z_C \frac{Z_{Lmax} + j * Z_c \tan(-\beta d_{max})}{Z_C + j * Z_{Lmax} \tan(-\beta d_{max})} \tag{8}$$

$$Z_L = Z_C \frac{Z_{Lmin} + j * Z_c \tan(-\beta d_{min})}{Z_C + j * Z_{Lmin} \tan(-\beta d_{min})}. \tag{9}$$

The sign of the phase is chosen to be negative because the origin of the coordinate system is

located at the load end. We can use (8) to compute the impedance if we utilize the voltage distribution, or (9) if we choose to employ the current distribution instead.

III. PLATFORM TOLERANCE STUDY OF TWO RFID TAGS

We will now present the results of the simulation of two different RFID tag antennas to illustrate the application of the approach for determining the tag impedance when we place the tags on different platforms. The two tags are: (i) PIFA [5], to which we add a loop near the feed point; and (ii) Meander Antenna [6], which is modified to render it to be more tolerant to the platforms by choosing its dielectric constant and thickness to be different from the one described in [6].
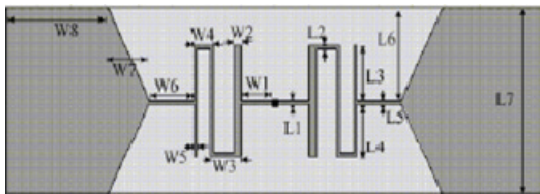
W1=4.5mm, W2=1mm, W3=4.5mm, W4=3mm, W5=0.5mm, W6=6.5mm, W7=6mm, W8=15mm, L1=0.5mm, L2=0.5mm, L3=7.25mm, L4=7.25mm, L5=0.5mm, L6=12.25mm, and L7=25mm.

(a)

0.5mm Copper

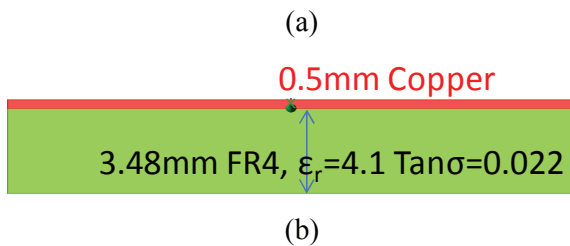3.48mm FR4, ε_r=4.1 Tanσ=0.022

(b)

Fig. 3.   Geometry of mender tag: (a) Top view; (b) Side view.

While placing the two tags on different types of materials, we introduce a 3 mm spacing between the tag and the material under test. Figure 5 shows the current distribution along the coax for the

PIFA. The vertical black and red lines indicate the locations of the ground plane and the dielectric substrate, respectively, along the coax for the PIFA case.
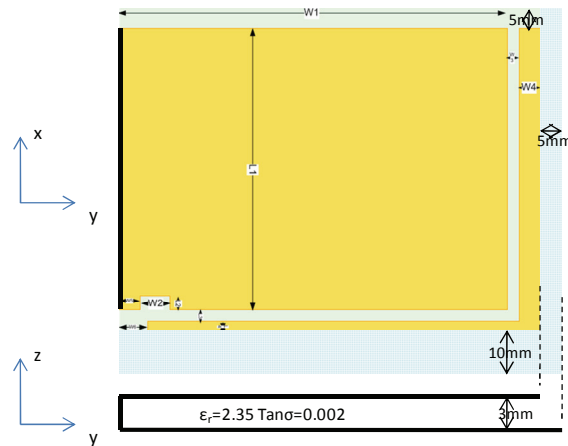
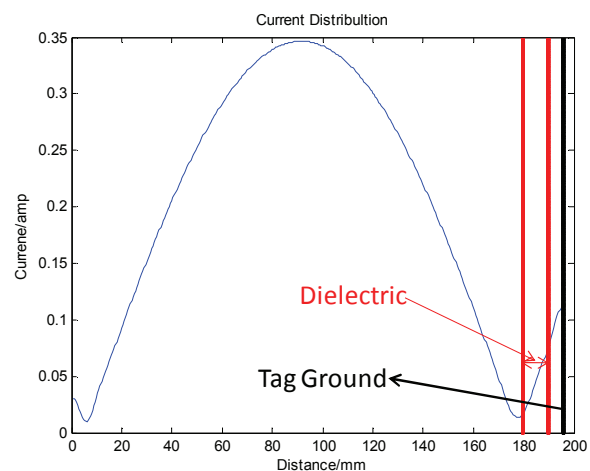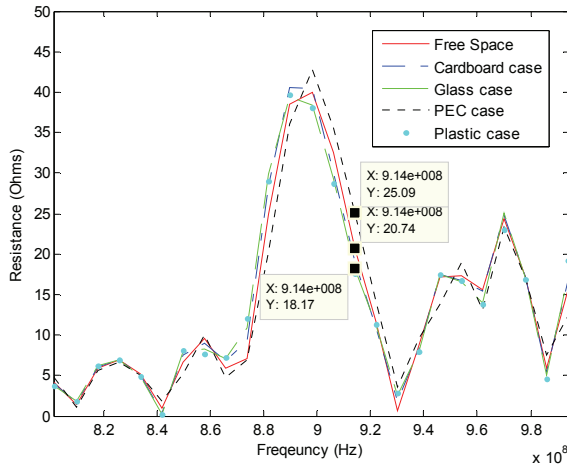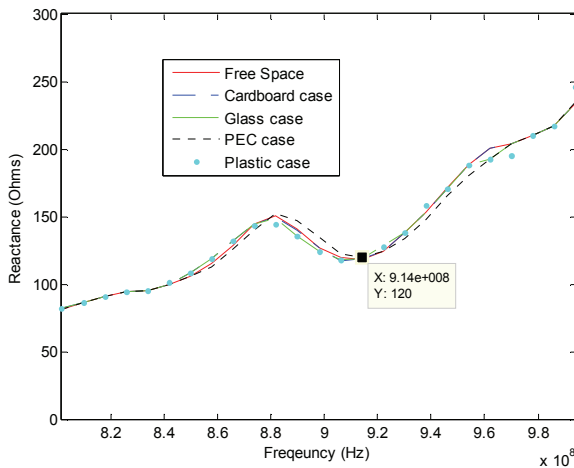| L=56.3mm	W1=53.2mm
L1=38.5mm	W2=4mm
L2=2mm	W3=1.6mm
L3=1.5mm	W4=3mm
L4=1.3mm	W5=3mm
W=62.8mm	W6=4mm

Fig. 4.   Geometry of PIFA tag.

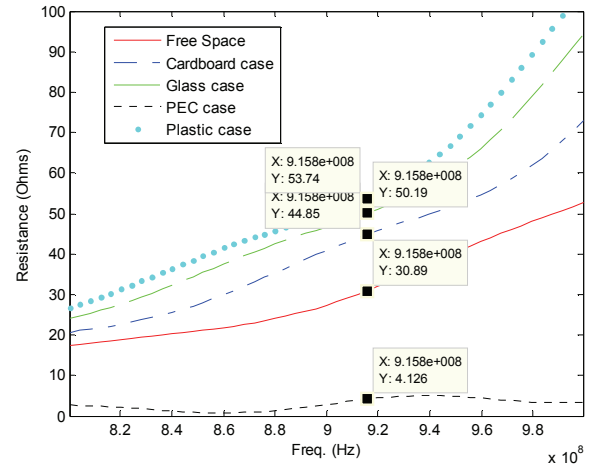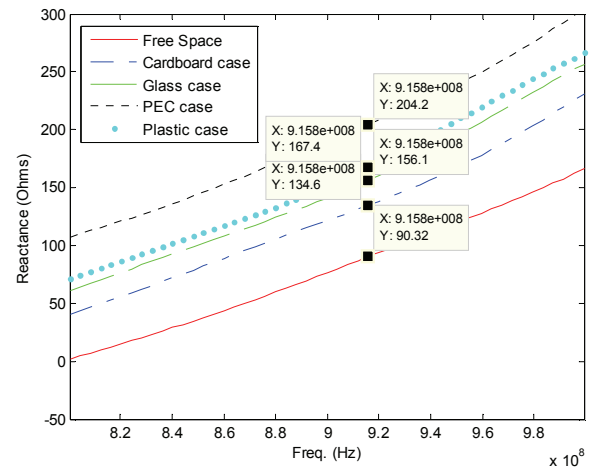Fig. 5.   Current distribution along longer coax fed for the PIFA tag.

(a)

(a)

(b)

(b)

Fig. 6. Input impedance of PIFA: (a) Resistance; (b) Reactance.

Fig. 7. Input impedance of meander tag antenna: (a) Resistance; (b) Reactance.

The simulation results for the real and imaginary parts of the input impedance are presented in Figs. 6 and 7 for the PIFA and the Meander tag antennas, respectively. These figures show that the tax provide a good conjugate-match to the IC impedance when located in a free space environment, since the real and imaginary parts of their input impedance are approximately is 30ohms and 100ohms, respectively. we also note that both put on the PEC background, the FIPA tag performs much better than the meander tag antenna, when they are placed on different

platforms, including a metallic one (PEC case). Figure 8 presents the return loss (RL) characteristics of the tags, calculated as follows

$$Return\ Loss = 20 * log10\left(\frac{Z_A(f) - Z_C(f)^*}{Z_A(f) + Z_C(f)}\right), \quad (9)$$

where Z_A and Z_C are the impedances of the antenna and the chip, respectively, both of which are frequency dependent. The RL plots clearly show that the presence of the ground underneath plays a critical role in shielding the tag from the material

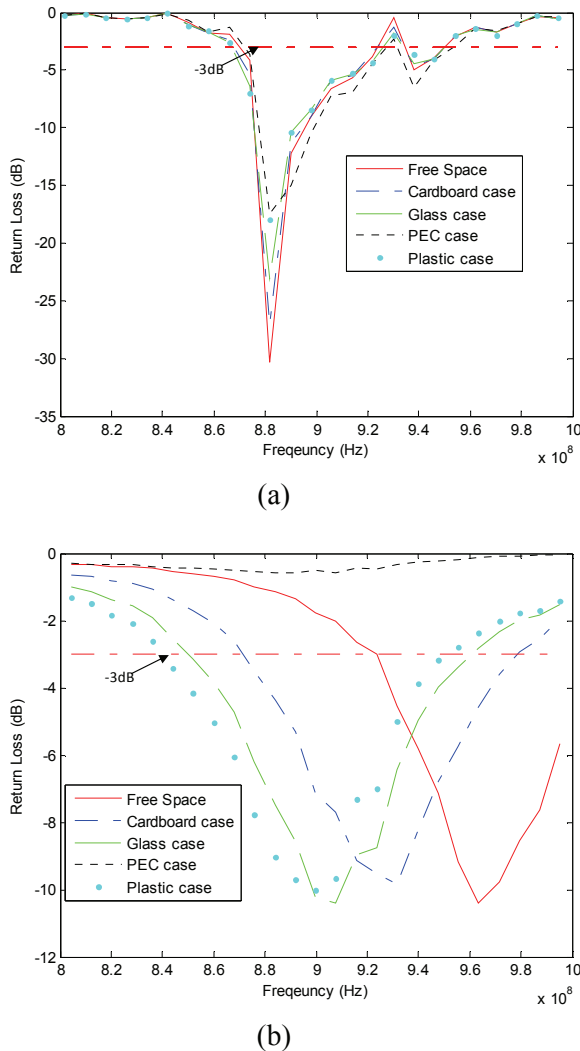below, and that the two tags perform differently from this perspective.

(a)

(b)

Fig. 8.   Return Loss Charcteristics of two tag antennas: (a) PIFA; (b) Meander tag.

IV. DISCUSSION OF RESULTS AND CONCLUSIONS

The platform tolerance of two types of tags have been investigated in this paper by using a novel simulation technique, described herein, which yields reliable and physically acceptable results for the input impedance, free of higher-order mode effects that are excited in the vicinity of the feed, and corrupt the impedance derived.

The simulation technique has been designed to mimic VNA measurements by using a coaxial line feed of sufficient length, rather than relying upon the conventional method of sampling the voltage and current at the feed point to compute the input impedance. Although the simulation could have been carried out by using either an FEM or MoM code, we have chosen to use a parallel version of the FDTD code, namely GEMS, because its superior ability to handle large, complex and multiscale problems over serial codes We have found that when the meander tag, which has no ground plane, is placed on cardboard (ε_r=2.5), glass (ε_r=3.8), and plastic (ε_r=4.7) [7], it performs reasonably well, its return loss remains below -3dB, and its impedance provides a good conjugate match the IC of chip of choice. However, this is no longer true when the same tag is placed on a metallic object. The tag performance is found to deteriorate significantly in this case, as may be clearly seen from Fig. 7a. In contrast to this, the PIFA tag continues to work well (see Fig.7b), not only when it is placed atop the three materials mentioned above, (cardboard, glass and plastic), but also when it is located above a metallic object, and its return loss remains better than -3dB for all of these scenarios. The PIFA exhibits a superior platform tolerance as compared to the Meander antenna because the former has its own built-in ground plane, which is larger than the footprint of the PIFA antenna itself by about 5*5*10 mm (see Fig.4). However, despite its larger dimensions, the improved performance of the PIFA antenna, described herein, justifies its use in preference to the Meander tag, especially in situations where the platform tolerance feature is important.

ACKNOWLEDGMENT

research was conducted, Li Li was in the Electromagnetic Communication Laboratory, Pennsylvania State University, University Park, PA 16802, as a visiting scholar.

REFERENCES

[1] P. V. Nikitin, K. V. S. Rao, and S. Lazar, "An Overview of Near Field UHF RFID," *IEEE International Coference on RFID,* March 2007.

[2] V. Chawla and D. Sam Ha, "An overview of passive RFID," *IEEE Applications & Practice,* Sep. 2007.

[3] P. V. Nikitin, K. V. S. Rao and R. D. Martinez, "Differential RCS of RFID tags," *Electronics letters* vol. 43, no. 8, April 2007.

[4] GEMS website: www.2comu.com.

[5] M. Hirvonen, K. Jaakkola, P. Pursula, and J. Saily, "Dual-Band Platform Tolerant Antennas for Radio-Frequency Identification," *IEEE Trans. Antennas Propagat.*, vol. AP-54, no. 9, pp. 2632-2637, Sept. 2006.

[6] S. -J. Wu and T. -G. Ma, "A passive UHF RFID Meandered Tag Antenna with Tuning Stubs," *Asia-Pacific Microwave Conference (APMC),* Dec. 2006.

[7] A. S. Hoenshel, "A Parametric Study on the Platform Tolerance of RFID Tag Antennas and Their Performance Enhancement with Artificial Magnetic Conductors" *M.S. Thesis,* Pennsylvania State University, 2007.